ISSN 1063-7826, Semiconductors, 2018, Vol. 52, No. 1, pp. 93–99. © Pleiades Publishing, Ltd., 2018.
Original Russian Text © S.A. Blokhin, M.A. Bobrov, A.A. Blokhin, A.G. Kuzmenkov, A.P. Vasil'ev, Yu.M. Zadiranov, E.A. Evropeytsev, A.V. Sakharov, N.N. Ledentsov, L.Ya. Karachinsky, A.M. Ospennikov, N.A. Maleev, V.M. Ustinov, 2018, published in Fizika i Tekhnika Poluprovodnikov, 2018, Vol. 52, No. 1, pp. 98–104.

PHYSICS OF SEMICONDUCTOR DEVICES

# Emission-Line Width and α-Factor of 850-nm Single-Mode Vertical-Cavity Surface-Emitting Lasers Based on InGaAs/AlGaAs Quantum Wells

**S. A. Blokhin[a]*, M. A. Bobrov[a], A. A. Blokhin[a], A. G. Kuzmenkov[b, a], A. P. Vasil'ev[b, a], Yu. M. Zadiranov[a], E. A. Evropeytsev[a], A. V. Sakharov[a], N. N. Ledentsov[c], L. Ya. Karachinsky[d, a], A. M. Ospennikov[e], N. A. Maleev[a], and V. M. Ustinov[b, a, f]**

[a] *Ioffe Institute, St. Petersburg, 194021 Russia*
[b] *Submicron Heterostructures for Microelectronics, Research and Engineering Center, Russian Academy of Sciences, St. Petersburg, 194021 Russia*
[c] *VI Systems GmbH, Berlin, Germany, D-10623*
[d] *Connector Optics LLC, St. Petersburg, 194292 Russia*
[e] *Russia Institute of Radionavigation and Time RIRT, St. Petersburg, 192012 Russia*
[f] *Peter the Great St. Petersburg Polytechnic University, St. Petersburg, 195251 Russia*
**e-mail: blokh@mail.ioffe.ru*

Submitted May 25, 2017; accepted for publication May 30, 2017

**Abstract**—The emission-line width for 850-nm single-mode vertical-cavity surface-emitting lasers based on InGaAs/AlGaAs quantum wells is studied. The width of the emission line for a laser with a 2-μm oxide current aperture attains it minimum (~110 MHz) at an output power of 0.8 mW. As the optical output power is further increased, anomalous broadening of the emission line is observed; this is apparently caused by an increase in the α-factor as a result of a decrease in the differential gain in the active region under conditions of increased concentration of charge carriers and of high internal optical losses in the microcavity. The α-factor is estimated using two independent methods.

**DOI:** 10.1134/S1063782618010062

## 1. INTRODUCTION

Semiconductor vertical-cavity surface-emitting lasers (VCSELs) with a spectral range of 850 nm are widely used both for the optical transmission of data and in various types of sensors and transducers [1]. Much attention is given to the issue of fabricating ultra-high-rate energy-efficient optical interconnections, in which it is necessary to increase the speed of response of lasers under conditions of their direct current modulation, to lower their energy consumption and simultaneously decrease the width of the laser-emission spectrum in order to reduce the signal's dispersion in the course of data transmission along the optical fiber [2, 3]. In recent years, interest has increased in microminiature sources of laser radiation based on VCSELs of the near-infrared (near-IR) range for applications in quantum magnetometers [4, 5], laser interferometers [6], and quantum frequency standards (so-called atomic clocks) [7, 8], where it is basically required that single-mode conditions for VCSEL laser generation with a fixed direction of polarization and a small width of the emission line be provided. The classical method for providing the single-mode condition for VCSEL generation is based on a decrease in the sizes of the current aperture used to limit the region of charge-carrier injection. In a VCSEL with a current aperture formed by the method of ion implantation, due to a small step in the effective refraction coefficient, there is no stable transverse optical confinement and the mode of laser emission is determined by thermal effects and/or by the spatial "burning" of holes while nonradiative recombination at radiation-induced defects brings about a sharp increase in the threshold current with a decrease in the aperture sizes. The above circumstances do not allow the implementation (by the mentioned method) of efficient single-mode fast-response lasers. The use of a current aperture obtained by the method of the selective oxidation of AlGaAs layers with a high content of Al makes it possible to provide an effective current and optical confinement without a significant increase in the internal optical losses [1]. In commercially available single-mode 850-nm VCSELs based on GaAs/AlGaAs quantum wells, the classical geometry of a microcavity with the injection of charge carriers through doped semiconductor distributed Bragg

reflectors (DBRs) and one oxide current aperture is typically used. In this case, the typical width of the line of laser generation amounts to ~100 MHz (at an output power of ~0.5 mW). An increase in the effective length of the microresonator and a decrease in losses by the extraction of radiation made it possible to decrease the width of the 850-nm VCSEL generation line to 23 MHz [9]. However, such an approach is accompanied by a decrease in the response time of the laser (as a result of an increase in the coefficient of damping of relaxation oscillations) and also by a decrease in the attainable level of the output optical power. Taking into account present-day trends in the development in VCSEL structures operating in the near IR region, as related to an increase in the differential gain in the active region (strained InAlGaAs active regions) and to a decrease in the parasitic capacitance (by the introduction of additional oxide layers, the pressing problem consists in an analysis of the width of the generation line for fast-response single-mode VCSELs based on strained InAlGaAs quantum-confinement heterostructures.

In this publication, we present the results of our experimental studies of single-mode polarization-stable VCSELs for the 850-nm spectral region; these VCSELs are based on InGaAs/AlGaAs quantum wells (QWs) in the classical configuration of a microcavity with an oxide current aperture. For these VCSELs, an anomalous behavior of the line width of generation at high levels of the output optical power is observed; an explanation for this effect is suggested and the value of the α-factor is estimated.

## 2. EXPERIMENTAL

The epitaxial structure of the 850-nm VCSELs under study is represented by a classical vertical microcavity with the vertical extraction of radiation and consists of a hidden $n^+$-GaAs contact layer, a lower doped distributed Bragg reflector (DBR) (the latter includes 35 pairs of the quarter-wave *n*-type $Al_{0.15}Ga_{0.85}As/Al_{0.9}Ga_{0.1}As$ layers), a 1-λ-AlGaAs microcavity with a strained InGaAlAs active region, the upper DBR including 22 pairs of quarter-wave *p*-type $Al_{0.15}Ga_{0.85}As/Al_{0.9}Ga_{0.1}As$ layers, and the surface contact *p*-type GaAs layer.

In order to ensure the fast capture of charge carriers and a small coefficient of gain compression, we used the structure of an optical microcavity with the separate confinement of charge carriers and with a gradient profile of the refraction coefficient. In order to increase the differential gain and suppress the thermal ejection of charge carriers, we used five layers of $In_{0.08}Ga_{0.92}As$ QWs, which have a thickness of 4 nm and are surrounded by AlGaAs barrier layers [10]. The number and thickness of the strained InGaAs QWs and also the thickness of the AlGaAs barrier layer are chosen such as to ensure the largest factor of optical confinement upon conservation of the position of the gain peak in the vicinity of 850 nm without significant deterioration in the structural and optical quality of the QW. In order to solve the problem of the transport of charge carriers through the DBR, we used gradient interfaces with a modulated profile of doping at the heteroboundaries of separate quarter-wave layers. Two aperture *p*-AlGaAs layers with a step-like composition profile (Al concentration) are located in the upper DBR in the immediate vicinity of the microcavity with the aim of reducing the parasitic capacitance of the VCSEL. The resonant wavelength of the microcavity is shifted to shorter wavelengths by 10 nm relative to the peak of gain in the active region (the so-called negative detuning of the gain spectrum relative to the resonance wavelength) with the aim of ensuring a high speed of response at room temperature.

The planar technology of VCSEL fabrication with classical configuration of the microresonator includes the following main operations: formation of an ohmic Ti/Pt/Au contact to the contact $p^+$-GaAs layer, etching of the mesa until the contact $n^+$-GaAs layer, formation of an oxide current aperture using selective oxidation of the aperture layer through opened portions at the walls of the mesa, the formation of an AuGe/Ni/Au contact to the contact $n^+$-GaAs layer, planarization of the developed surface by bisbenzocyclobutene (BCB), and the formation of *n*- and *p*-type contact areas in the high-frequency topology. In order to attain a compromise between a high speed of response of the lasers in the mode of direct current modulation, the maintenance of low threshold currents, and a high differential efficiency, the reflection coefficient of the upper mirror was optimized experimentally via shallow etching of the DBR near-surface layer [11].

The actual size of the current oxide aperture for each VCSEL under study was verified by two methods: by analysis of the near-field pattern in the subthreshold mode of laser operation and by analyzing the contrast of the refractive indices at the oxide–semiconductor interface in the case of IR illumination. As a result of the slight anisotropy of selective oxidation of the AlGaAs layers with a high content of Al, the oxide current aperture has a shape close to a quadratic one [12]. It was found that the region of spontaneous electroluminescence at a low pump-current level well falls within the limits of the region determined by the boundaries of the contrast of the refractive indices for the oxide–semiconductor interface. Apparently, this is due to the fairly homogeneous injection of charge carriers into the active region as a result of the presence of additional potential barriers at the heteroboundaries of the relatively low-doped DBR layers in the vicinity of the microcavity. The dynamic characteristics of the VCSELs were studied using a microwave probe directly at the wafer. For studies of the polarization and for measurements of the emission

line width, individual lasers were mounted in test cases (in order to reduce the effect of mechanical stresses from the probe contacts).

## 3. RESULTS AND DISCUSSION

The use of several oxide aperture layers in order to reduce the capacitance of a VCSEL gives rise to an increase in the waveguide effect in the transverse direction due to an increase in the contrast of the effective refraction index at the outer boundaries of the active region; as a result, multimode laser generation via the transverse Laguerre–Gauss modes arises in the lasers with a characteristic size of the oxide current aperture of larger than 3 μm.

Figure 1 shows the power–current ($W$–$I$) and spectral characteristics of a VCSEL with a characteristic size of the current aperture amounting to ~2 μm; the characteristics were measured in the continuous mode of operation at room temperature. Laser generation at about 860 nm with a threshold current of ~0.56 mA, a differential efficiency of ~0.65 W/A, and maximal output optical power of ~1.75 mW at a current of 5 mA was implemented in the VCSELs under consideration. According to the results of analysis of the evolution of the generation spectra with current and temperature, the thermal resistance of the lasers is as high as 7 K/mW due to the fairly low thermal conductivity of the lower DBR (~25 W $m^{-1}$ $K^{-1}$). As the pump current is increased, thermal effects caused by self-heating of the laser (thermal lens, drop in the gain) bring about a decrease in the efficiency of selection of the fundamental mode. Nevertheless, single-mode generation with a side-mode suppression ratio (SMSR) of >30 dB is retained in the entire range of pump currents. Despite degeneration of the fundamental mode over polarization, studies of polarization revealed the predominance of the selected direction of emission polarization for a VCSEL with an orthogonal-polarization suppression ratio (OPSR) of >15 dB within the entire operating range of currents without any polarization switching. This is apparently caused by the electro-optical effect or mechanical stresses in combination with the complex shape of the oxide current aperture [13, 14].

Taking into account the Schawlow–Townes relation [15] and the features of the behavior of the refractive index in semiconductor injection lasers [16], the width of the emission line for a single-mode VCSEL can be expressed as

$$\Delta\nu_L^{ST} = \frac{\Gamma R'_{\mathrm{sp}}}{4\pi N_p}(1+\alpha^2), \quad (1)$$

where $N_p$ is the concentration of photons in the mode under consideration (i.e., the total number of photons $n_p$ (in this mode) in relation to the volume $V_p$ of the mode; in the case under consideration, this volume is

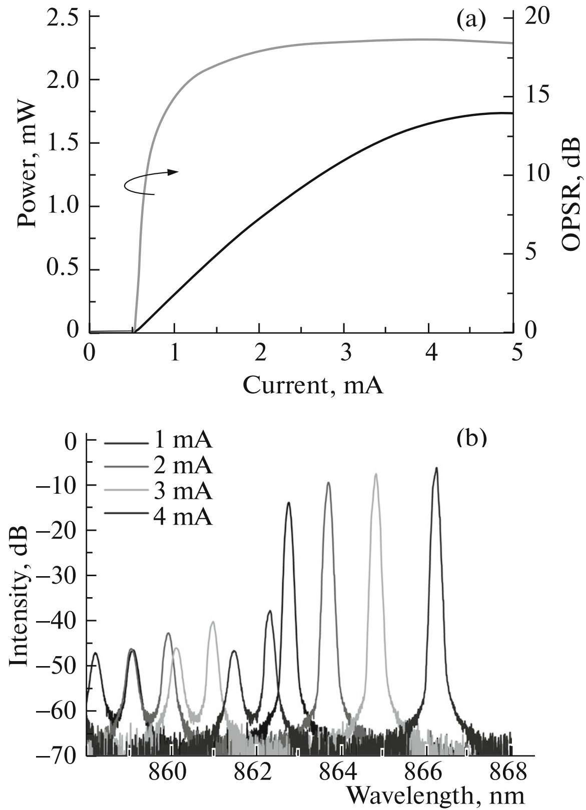


**Fig. 1.** VCSEL with a characteristic size of the current aperture (2 μm): (a) power–current characteristic and the dependence of the OPSR factor of suppression of the orthogonal polarization on the pump current and (b) the spectra of laser generation at different pump currents. The measurements were performed at room temperature.

assumed to be equal to that of the microcavity); $R'_{\mathrm{sp}}$ is the rate of spontaneous emission related to this mode (i.e., the number of photons emitted spontaneously to the mode under consideration per unit time and related to the volume $V_a$ of the active region); Γ is the three-dimensional factor of optical confinement (in what follows, the Γ-factor); and α is the factor of the broadening of a spectral line (in what follows, the α-factor). The concentration of photons $N_p$ and the rate of spontaneous emission $R'_{\mathrm{sp}}$ at the generation threshold can be represented in the following form [17]:

$$N_p = P/h\nu V_p v_g g^*_{\mathrm{th}}\eta_0, \quad (2)$$

$$R'_{\mathrm{sp}} = v_g g^*_{\mathrm{th}} n_{\mathrm{sp}}/V_a. \quad (3)$$

Here, $P$ is the output optical power, $h\nu$ is the energy of photons emitted at the resonance wavelength of the mode under consideration, $v_g$ is the group velocity (~8.5 × $10^9$ cm/s), $g^*_{\mathrm{th}}$ is the modal threshold gain, $\eta_0$ is the external quantum efficiency, and $n_{\mathrm{sp}}$ is the factor of inverse population (typically, ~1.5). Since the

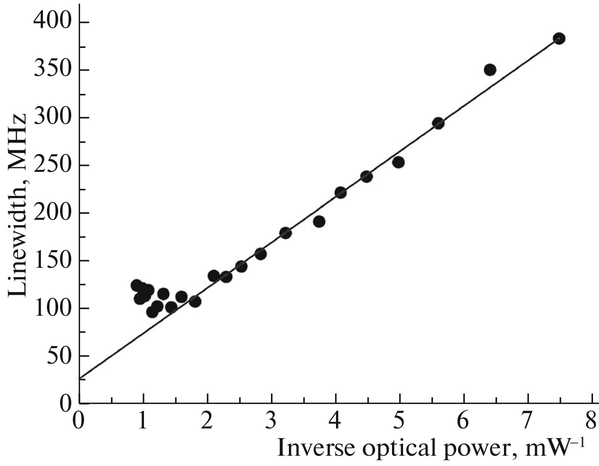


**Fig. 2.** Dependence of the width of the emission line for a VCSEL with a characteristic size of the current aperture (~2 μm) on the reciprocal value of the output optical power. The measurements were performed at room temperature.

Γ-factor is expressed in terms of volumes of the active region and the mode as $\Gamma = V_a/V_p$, expression (1) can be rewritten as

$$\Delta\nu_L^{ST} = \frac{h\nu(v_g g_{\text{th}}^*)^2 n_{\text{sp}}\eta_0}{4\pi P}(1+\alpha^2). \tag{4}$$

Figure 2 shows the results of measurements of the emission-line width $\Delta\nu_L$ for a VCSEL with a characteristic size of the current aperture of about 2 μm; the results were obtained using a Thorlabs SA-200 Fabry–Perot scanning interferometer with a resolving power of 7.5 MHz. In order to suppress noise caused by instability of the power supply and by parasitic optical feedback, we used a chemical power supply and an optical insulator was introduced between the laser and the interferometer. Two portions can be discerned in the experimental dependence of the width of the VCSEL's generation line on the level of the reverse output optical power. In the first portion, the width of the emission line decreases with an increase in the optical power. However, as the optical power is increased further (in the second portion), a large deviation of $\Delta\nu_L$ from the linear dependence is observed; this effect can also bring about a broadening of the generation line in single-mode VCSELs in the case of direct current modulation [18]. As a result, the width of the emission line for the VCSELs under study attains its smallest value ~110 MHz at an output optical power of 0.8 mW (at an operating current of 1.8 mA); this is the value typical for a VCSEL with classical geometry of the microcavity (without a substantial increase in its effective length) [8, 19].

The width of the emission line for a VCSEL is inversely proportional (in the first portion) to the output power, which correlates with expression (4); however, the extrapolation of such a dependence in the case where the optical power tends to infinity yields a nonzero value of the emission line width: $\Delta\nu_0 \approx$ 40 MHz (the so-called residual emission line width). Apparently, this fact can be either caused by the competition of transverse modes or be related to flicker noise due to a fluctuation in the mobility of charge carriers [20]. As a result, the expression (for the VCSEL emission line width) adequately describing the experimental results is written as

$$\Delta\nu_L = \Delta\nu_L^{ST} + \Delta\nu_0. \tag{5}$$

In order to estimate the α-factor, it is necessary to calculate the values of the parameters $g_{\text{th}}^*$ and $\eta_0$. The modal threshold gain compensates the sum of internal optical losses and the total losses related to the extraction of radiation through both mirrors of the microcavity $T_m = -\ln(R_F R_B)/2L_{\text{eff}}$, where the effective length $L_{\text{eff}}$ (~1.5 μm) accounts for the final depth of penetration of an electromagnetic field into the DBR. Since the reflectivity of the lower (dummy) DBR in the experiment is always smaller than 100%, it is necessary to introduce a correction $F$, which represents the fraction of the optical power leaving through the upper (output) DBR:

$$F = \left(\frac{\sqrt{R_B}}{\sqrt{R_F}+\sqrt{R_B}}\right)\left(\frac{1-R_F}{1-\sqrt{R_F R_B}}\right). \tag{6}$$

As a result, the external quantum efficiency can be written as

$$\eta_0 = \frac{\eta_d^F}{F\eta_j}\frac{e}{h\nu}, \tag{7}$$

where $\eta_d^F$ is the differential efficiency of the extraction of emission through the upper DBR, $\eta_i$ is the internal quantum efficiency (the so-called efficiency of current injection), and $e$ is the elementary charge. Calculations of the coefficients of reflection from the upper and lower DBRs in the context of the method of transport matrices produce the values $R_F \approx 98.9\%$ and $R_B \approx 99.99\%$, which makes it possible to estimate the values of $F$ and $T_m$ as $F \approx 0.99$ and $T_m \approx 37$ cm$^{-1}$. The internal optical losses and internal quantum efficiency can be determined in the context of the approach described by Yang et al. [21]. In the case under consideration, for the single-mode VCSELs under study, we observe an increase in the internal optical losses $A_{\text{int}}$ to 21 cm$^{-1}$ and a decrease in the efficiency of current injection to ~70% as compared with wide-aperture devices due to the diffuse scattering of light at oxide layers and to an increase in the loss of charge carriers at their increased concentration. Substituting (7) into (4) and taking into account the relation (5), we obtain a value of ~3.4 for the α-factor, which is consistent with similar estimations of the α-factor for a VCSEL with an active region

based on a GaAs/AlGaAs QW [19] and on strained $In_{0.2}Ga_{0.8}As$/GaAs QWs [22].

Anomalous broadening of the emission line as the power is increased was previously observed for single-mode VCSELs, which emitted in the spectral range around 1.55 μm and were based on a tunneling junction [23], and was attributed to the nonlinearity of the gain in the presence of competing modes [24]. However, in the case under consideration, the pronounced waveguide effect at the oxide current aperture brings about a fixing of the mode composition of the laser and leads to the formation of a unified reservoir of charge carriers for transverse modes. The observed anomalous behavior of the emission line width within the second portion of the $\Delta\nu_L(P)$ dependence is apparently related to an increase in the α-factor upon an increase in the output power under conditions of a high density of charge carriers and photons in the microcavity [25]. In fact, the α-factor is equal to the ratio of variations in the real and imaginary parts of the complex refractive index of the active region of the laser and can be represented as [16, 17]

$$\alpha = \frac{4\pi}{\lambda}\frac{\partial n/\partial N}{\partial g/\partial N}, \quad (8)$$

where $\lambda$ is the wavelength of laser emission, $\partial n/\partial N$ is the variation in the real part of the refractive index in the active region as the concentration of charge carriers is varied, and $\partial g/\partial N$ is the variation in the gain of the active region as the concentration of charge carriers is varied (differential gain).

According to [26], the variation in the refractive index of the active region caused by a variation in the concentration of charge carriers under conditions of continuous pumping can be determined from an analysis of the behavior of the VCSEL wavelength in relation to the current (see Fig. 3). The observed shift of the resonance wavelength $\Delta\lambda$ constitutes the superposition of a short-wavelength shift of the resonance wavelength $\Delta\lambda_{AR}$ (this shift is caused by a variation in the refractive index of the active region) and the long-wavelength shift of the resonance wavelength $\Delta\lambda_{SH}$, which is caused by self-heating of the laser. Since, in the first approximation, the concentration of charge carriers is fixed at the threshold of generation, the actual shift $\Delta\lambda_{SH}$ can be determined from analysis of the shift of the resonance wavelength with dissipated power $P_{dis}$ above the generation threshold (in the case under consideration, $\partial\lambda/\partial P_{dis} \approx 0.42$ nm/mW). Figure 3 also shows the dependence of the shift $\Delta\lambda_{AR}$ on the current $I$ for the VCSEL under study; according to [27], this dependence can be approximated by the following expression:

$$\Delta\lambda_{AR} = -k[\sqrt{I/I_{th}} - 1]. \quad (9)$$

Here, $k = 1.35$ nm is the resulting shift of the resonance wavelength when the threshold current $I_{th}$ is attained; this shift is caused by a variation in the refractive index of the active region. Then, the variation in the refractive index of the active region with the concentration of charge carriers can be determined from the expression [26]

$$\frac{\partial n}{\partial N} = \frac{k n_{eff} L_{eff}}{\lambda d_a N_{th}}, \quad (10)$$

where $n_{eff}$ is the effective refractive index (~3.5), $d_a$ is the total thickness of the active region, and $N_{th}$ is the threshold concentration of charge carriers in the active region; the latter concentration can be calculated using expression [17]

$$N_{th} = \frac{\eta_i I_{th} \tau_{sp}}{e V_a}, \quad (11)$$

where $\tau_{sp}$ is the lifetime of charge carriers up to the threshold. Unfortunately, the published data on the lifetime of charge carriers in strained InGaAs QWs differ rather widely. For example, according to [28], the value of $\tau_{sp}$ for an InGaAs QW depends only slightly on the In content (within 5–15%) and amounts to ~0.5 ns. However, the profound effect of the height of potential barriers on the value of $\tau_{sp}$ for an $In_{0.2}Ga_{0.8}As$/AlGaAs QW was detected in [29]; as a result of this effect, $\tau_{sp}$ increased from ~0.9 to ~4.2 ns as the Al content decreased from 20% to 0%. In order to obtain reliable data, we fabricated a test heterostructure with an active region similar to that in the VCSEL under study; the lifetime of charge carriers was measured in this heterostructure by the method of the time-resolved photoluminescence spectroscopy. An analysis of the decay time for the photoluminescence made it possible to estimate the lifetime of charge carriers in the $In_{0.08}Ga_{0.92}As$/AlGaAs QW at a level of ~1.3 ns. According to expression (11), the threshold concentration of charge carriers in the active region in the VCSEL under study attains a value of $\sim 3.3 \times 10^{19}$ cm$^{-3}$. Calculation of the variation in the refractive index of the active region with a change in the concentration of charge carriers according to expression (10) yields a value of $\sim 5.6 \times 10^{-21}$ cm$^3$, which is appreciably smaller than the published data for strained $In_{0.2}Ga_{0.8}As$/GaAs QWs but is quite consistent with the data for the GaAs/AlGaAs QWs [28].

The differential gain of the active region in the VCSEL under study can be determined from the results of small-signal frequency analysis. Figure 4 shows the dependence of the resonance frequency (or the frequency of relaxation oscillations) on the pump current; this dependence was obtained by approximation of the experimental amplitude–frequency characteristics in the context of the standard model for the frequency response of an injection laser. The rate of increase in the resonance frequency with increasing

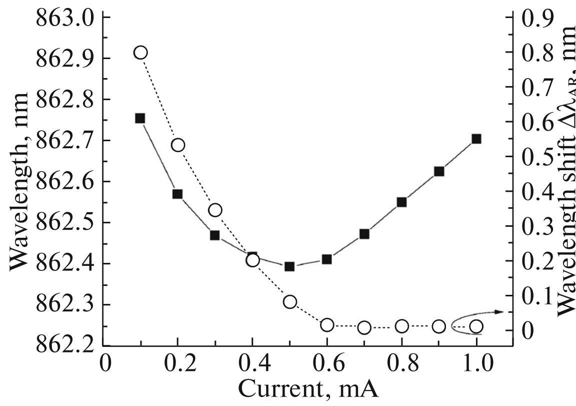


**Fig. 3.** Dependences of the resonance wavelength and the shift of the resonance wavelength $\Delta\lambda_{AR}$ (caused by a variation in the refractive index of the active region) on the pump current for a VCSEL with a characteristic size of the current aperture of ~2 μm. The measurements were performed at room temperature.

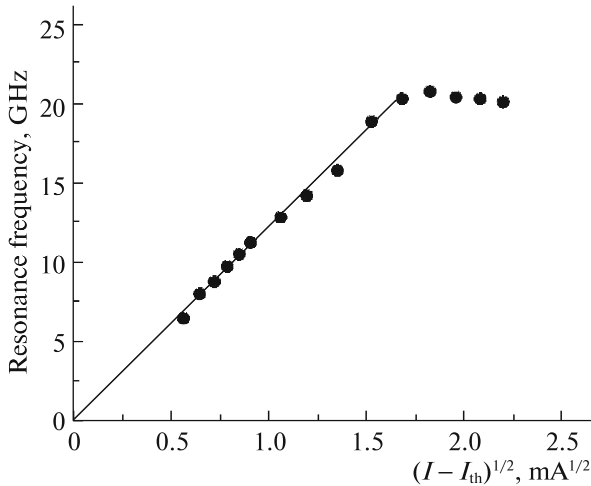


**Fig. 4.** Dependence of the resonance frequency on the pump current $\sqrt{I - I_{\text{th}}}$ for a VCSEL with a characteristic size of the current aperture of ~2 μm. The measurements were performed at room temperature.

current (the so-called *D*-factor) equals ~12 GHz/mA$^{1/2}$ and, according to [19], can be written as

$$D = \frac{1}{2\pi}\sqrt{\frac{\eta_i v_g}{eV_p}(\partial g/\partial N)}. \quad (12)$$

Using the approach to the estimation of the mode volume [31], we can estimate the differential gain of the active region as ~$2.7 \times 10^{-16}$ cm$^2$, which is approximately three times smaller compared with the results of similar estimations for wide-aperture lasers [11]. Calculation of the α-factor using expression (8) results in a value of three which is quite consistent with estimates of the α-factor on the basis of the laser-emission line width. However, the differential gain depends both on the concentration of charge carriers and on the spectral mismatch of the gain spectrum and the resonance wavelength [22]. On the one hand, a shift of the resonance wavelength brings about a decrease in the differential gain and, as a consequence, gives rise to an increase in the α-factor. On the other hand, a shift of the resonance wavelength to shorter wavelengths in the gain spectrum (relative to the peak) at a fixed concentration of charge carriers gives rise to an increase in the differential gain and, as a result, brings about a decrease in the α-factor. A decrease in the gain requires an increase in the concentration of charge carriers for attaining the generation threshold, thereby partially compensating the decrease in the α-factor. Thus, a small volume of the microcavity (a small size of the current aperture) under conditions of high internal losses gives rise to a high concentration of charge carriers in the microcavity, which, in turn rapidly transfers the laser to the mode of gain saturation with increasing pumping current and gives rise to an increase in the α-factor, which brings about a broadening of the emission line.

## 4. CONCLUSIONS

In this study, we investigated in detail single-mode VCSELs of the spectral range near 850 nm; the lasers were based on InGaAs/AlGaAs QWs and had a characteristic size of the current aperture amounting to ~2 μm. In the lasers, we obtained single-mode laser generation with large (>15 dB) suppression of the orthogonally polarized mode. The width of the laser emission line at first decreases in inverse proportion to an increase in the output optical power and attains its minimum (~110 MHz) at 0.8 mW. However, under conditions of increased concentration of charge carriers in the microcavity (due to its small size and high internal optical losses), the laser transfers to the mode of gain saturation, which brings about a decrease in the differential gain with increasing pump current, an increase in the α-factor, and an increase in the emission line width.

We estimated the value of the α-factor using two methods. Estimation of the α-factor from experimental dependence of the emission line width on the optical power taking into account the residual emission line width ($\Delta\nu_0 \approx 40$ MHz) yields a value of ~3.4. Estimation of the α-factor on the basis of values of the variation in the refractive index in the active region as a function of the concentration of charge carriers and differential gain of the active region yields a value of ~3. Close values of the α-factor obtained by two independent methods make it possible to conclude that the obtained estimates are adequate. The revealed effects and obtained data can be used for subsequent optimization of the structure of single-mode VCSELs

with the aim of minimization of the laser emission line width.


## ACKNOWLEDGMENTS

The studied lasers are the result of a joint project between VI Systems GmbH and Connector Optics LLC.


## REFERENCES


1. R. Michalzik, *VCSELs: Fundamentals, Technology and Applications of Vertical-Cavity Surface-Emitting Lasers* (Springer, Berlin, 2013).
2. P. Moser, P. Wolf, G. Larisch, H. Li, J. A. Lott, and D. Bimberg, Proc. SPIE **9001**, 900103 (2014).
3. E. Haglund, P. Westbergh, J. S. Gustavsson, E. P. Haglund, A. Larsson, M. Geen, and A. Joel, Electron. Lett. **51**, 1096 (2015).
4. P. D. D. Schwindt, B. Lindseth, S. Knappe, V. Shah. J. Kitching, and L.-A. Liew, Appl. Phys. Lett. **90**, 081102 (2007).
5. M. Prouty and A. Miniature, *Wide Band Atomic Magnetometer, SERDP Project MR-1568* (Geometrics Inc., 2011).
6. A. Pruijmboom, M. Schemmann, J. Hellmig, J. Schutte, H. Moench, and J. Pankert, Proc. SPIE **6908**, 69080I (2008).
7. L. Knappe, V. Shah, P. D. D. Schwindt, L. Hollberg, J. Kitching, L. A. Liew, and J. Moreland, Appl. Phys. Lett. **85**, 1460 (2004).
8. D. K. Serkland, K. M. Geib, G. M. Peake, R. Lutwak, A. Rashed, M. Varghese, G. Tepolt, and M. Prouty, Proc. SPIE **6484**, 648406 (2007).
9. D. K. Serkland, G. A. Keeler, K. M. Geib, and G. M. Peake, Proc. SPIE **7229**, 722907 (2009).
10. S. B. Healy, E. P. O'Reilly, J. S. Gustavsson, P. Westbergh, E. Haglund, A. Larsson, and A. Joel, IEEE J. Quantum Electron. **46**, 506 (2010).
11. M. A. Bobrov, S. A. Blokhin, N. A. Maleev, A. G. Kuzmenkov, A. A. Blokhin, Yu. M. Zadiranov, S. I. Troshkov, N. N. Ledentsov, and V. M. Ustinov, J. Phys.: Conf. Ser. **643**, 012044 (2015).
12. K. D. Choquette, K. M. Geib, C. I. H. Ashby, R. D. Twesten, O. Blum, H. Q. Hou, D. M. Follstaedt, B. E. Hammons, D. Mathes, and R. Hull, IEEE J. Sel. Top. Quant. Electron. **3**, 916 (1997).
13. M. P. van Exter, A. K. Jansen van Doorn, and J. P. Woerdman, Phys. Rev. A **56**, 845 (1997).
14. F. Monti di Sopra, M. Brunner, and R. Hövel, Photon. Technol. Lett. **14**, 1034 (2002).
15. A. L. Schawlow and C. H. Townes, Phys. Rev. **112**, 1940 (1958).
16. C. H. Henry, IEEE J. Quant. Electron. **18**, 259 (1982).
17. K. Petermann, *Laser Diode Modulation and Noise* (Kluwer Academic, Dordrecht, 1991).
18. N. N. Ledentsov, J. A. Lott, J.-R. Kropp, V. A. Shchukin, D. Bimberg, P. Moser, G. Fiol, A. S. Payusov, D. Molin, G. Kuyt, A. Amezcua, L. Y. Karachinskiy, S. A. Blokhin, I. I. Novikov, N. A. Maleev, C. Caspar, and R. Freund, Proc. SPIE **8276**, 82760K (2012).
19. D. Kuksenkov, S. Feld, C. Wilmsen, H. Temkin, S. Swirhun, and R. Leibenguth, Appl. Phys. Lett. **66**, 277 (1995).
20. L. A. Coldren, S. W. Corzine, and M. L. Mašanović, *Diode Lasers and Photonic Integrated Circuits* (Wiley, New York, 2012).
21. G. M. Yang, M. H. Mac Dugal, V. Pudikov, and P. D. Dapkus, Photon. Technol. Lett. **7**, 1228 (1995).
22. D. Summers, P. Dowd, I. H. White, and M. R. T. Tan, Photon. Technol. Lett. **7**, 736 (1995).
23. A. Bacou, A. Rissons, and J.-C. Mollier, Proc. SPIE **6908**, 69080F (2008).
24. KU. Krüger and K. Petermann, IEEE J. Quant. Electron. **24**, 2355 (1988).
25. H. Halbritter, R. Shau, F. Riemenschneider, B. Kögel, M. Ortsiefer, J. Rosskopf, G. Böhm, M. Maute, M.-C. Amann, and P. Meissner, Electron. Lett. **40**, 1266 (2004).
26. K. Kishino, S. Aoki, and Y. Suematsu, J. Quant. Electron. **18**, 343 (1982).
27. K. Stubkjaer, Y. Suematsu, M. Asada, S. Arai, and A. R. Adams, Electron. Lett. **16**, 895 (1980).
28. M. H. Moloney, J. Hegarty, L. Buydens, P. Demeester, R. Grey, and J. Woodhead, Appl. Phys. Lett. **62**, 3327 (1993).
29. A. P. Ongstad, D. J. Gallant, and G. C. Dente, Appl. Phys. Lett. **66**, 2730 (1995).
30. M. Usami, H. Sakata, and Y. Matsushima, in *Proceedings of the 19th International Symposium on Gallium Arsenide and Related Compounds, 1992*, p. 803.
31. C. H. Wu, F. Tan, M. Feng, and N. Holonyak, Jr., Appl. Phys. Lett. **97**, 091103 (2010).


*Translated by A. Spitsyn*